

See discussions, stats, and author profiles for this publication at: <https://www.researchgate.net/publication/341536062>

Operational Efficiency Improvement of PEM Fuel Cell – A Sliding Mode Based Modern Control Approach

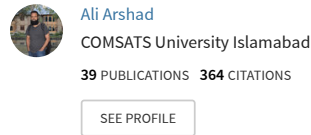
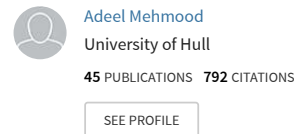
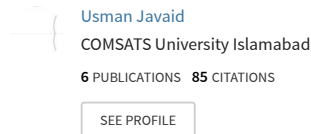
Article in IEEE Access · May 2020

DOI: 10.1109/ACCESS.2020.2995895

CITATIONS
22

READS
362

5 authors, including:



Received April 29, 2020, accepted May 7, 2020, date of publication May 20, 2020, date of current version June 3, 2020.

Digital Object Identifier 10.1109/ACCESS.2020.2995895

Operational Efficiency Improvement of PEM Fuel Cell—A Sliding Mode Based Modern Control Approach

USMAN JAVAID^{ID1}, ADEEL MEHMOOD¹, ALI ARSHAD^{ID1}, (Member, IEEE), FAHAD IMTIAZ^{1,4}, AND JAMSHED IQBAL^{ID2,3}, (Senior Member, IEEE)

¹Department of Electrical and Computer Engineering, COMSATS University Islamabad, Islamabad 45550, Pakistan

²Department of Electrical Engineering, National University of Computer and Emerging Sciences (FAST-NU), Islamabad 44000, Pakistan

³Department of Electrical and Electronic Engineering, College of Engineering, University of Jeddah, Jeddah 21589, Saudi Arabia

⁴KSA Branch, Metallurgical Corporation of China, COMSATS University Islamabad (CUI), Islamabad 45550, Pakistan

Corresponding author: Usman Javaid (usman_javaid@comsats.edu.pk)

ABSTRACT The efficiency and durability of a Proton Exchange Membrane Fuel Cell (PEMFC) can be improved with proper controller design to regulate the flow of reactants, cell stack temperature and humidity of the membrane. In this paper, sliding mode controllers (SMC) are proposed for a *polymer electrolyte membrane fuel cell* PEMFC. In particular, first order SMC and second order SMC based on super twisting algorithm are designed and investigated. The actual process has been formulated in simulation by Pukurushpan's ninth order model. Performance of both control laws has been compared in simulation in MATLAB/Simulink environment in terms of oxygen excess ratio, net power generated, stack voltage/power produced and compressor motor voltage. Simulation results dictate that second order SMC demonstrates superior performance in terms of set-point tracking and disturbance rejection. The designed controller makes the interaction of various subsystems in a smooth manner and consequently improves the overall efficiency of the system and prolongs the stack life of the fuel cells.

INDEX TERMS Efficiency improvement, oxygen excess ratio, PEM fuel cell, sliding mode control, super twisting algorithm.

I. INTRODUCTION

Energy demand is increasing with the passage of time [1]. With exponential population growth, the demand of energy is also increasing exponentially. Nowadays, almost each and every aspect of human life is partially or completely dependent on energy. Unlike other living organisms, humans have been successful in discovering and developing different kinds of fuels to fulfil their energy needs [2]. Energy crisis is the greatest threat that can ever be faced by human civilization. Also the rapid advancements in technology and industry is anticipated to lead to energy crisis.

Fossil fuels are the main source of energy which meet up-to 80% of our total energy requirements. The expansion of population and economies of most nations in the past century has been facilitated by increase in the use of fossil fuels [3]. About 70% of electrical energy requirements

The associate editor coordinating the review of this manuscript and approving it for publication was Navanietha Krishnaraj Krishnaraj Rathinam.

around the world is produced from fossil fuels, also majority of transportation systems use internal combustion engines. With increasing population, the consumption of fossil fuels has also increased exponentially over time, thereby depleting them rapidly. The combustion of fossil fuels produces carbon dioxide, carbon monoxide and nitrogen oxide and a lot of energy is dissipated in the form of heat. These oxides and un-burned hydrocarbons are a major health hazard for human being and also cause an overall negative impact on our environment. Moreover, animals and plants are facing new challenges for their survival due to emission of these gases [4]. Melting glaciers, rising water levels in seas, heavy rains in some areas and intense droughts and heat waves in some other areas are the penalties of global warming and climatic changes [5]. Unburned hydrocarbons and different oxides of Nitrogen emitted by the combustion engines are the main causes of smog formation, ozone layer damage and acid rains [6]. It is reported in [7] that 37 billion tons of carbon dioxide is emitted worldwide in year 2019 due

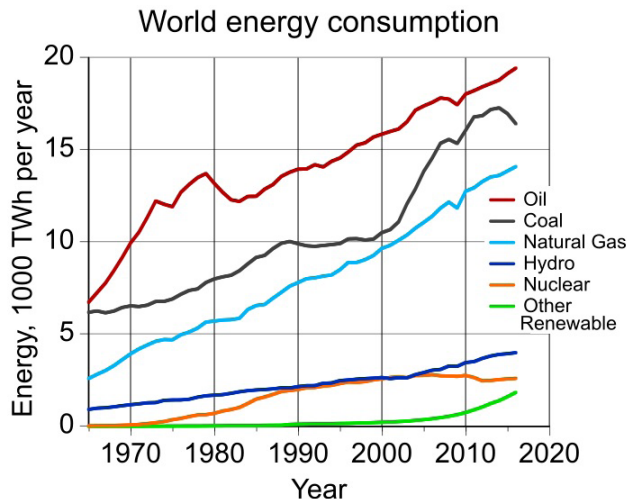


FIGURE 1. World's energy consumption trend.

to burning of coal, oil and other fossil fuels. The demand of fossil fuels is increasing since past 30 years as depicted in figure 1. This demand is expected to increase even more with the passage of time [8] and if this trend of fossil fuel consumption continues, then over next 35 to 37 years, the earth is going to run out of stock [9]. In order to cope with receding fossil fuels and their impact on our environment and health, various strategies are being considered. For example, algal fuels concept is a way of producing ‘carbon neutral’ fuel from renewable energy resources. The concept is 50 years old, however its commercialization has not been achieved due to economical challenges [10]. Alternatively, other renewable energy resources like solar cells and wind turbines produce fluctuating energy and efforts are being made for their smooth energy production [11]. There are limitations like e.g. wind is not blowing at equal speeds all the times and the sun does not shine with the uniform intensity throughout the day [12]. Hydroelectric power generation is also a good renewable source of energy production. Recently, studies have been conducted on Archimedes screw generator, which were historically used as pumps, to improve the efficiency of power production [13]. However, hydroelectric energy production is location dependent and is not suitable to be used in transportation or in portable applications.

Intensive studies have been done on PEMFCs to demonstrate that they are eco-friendly and efficient energy source for stationary as well as portable applications [14]. The PEMs is the key component of PEMFC and involves protons transfer from anode to cathode. The reactant gas is blocked and electrons are generated [15]. Hydrogen acts as the primary fuel and thus the hydrogen production is the key process for the fuel cell to produce energy. There are three types of electrolysis classified by ion transfer Acidic (PEM) electrolyzers, alkaline (AEL) and solid oxide electrolyzers(SOEC) [16]. The membranes of PEM fuel cells have various drawbacks including low glass transition heat, poor thermal and mechanical

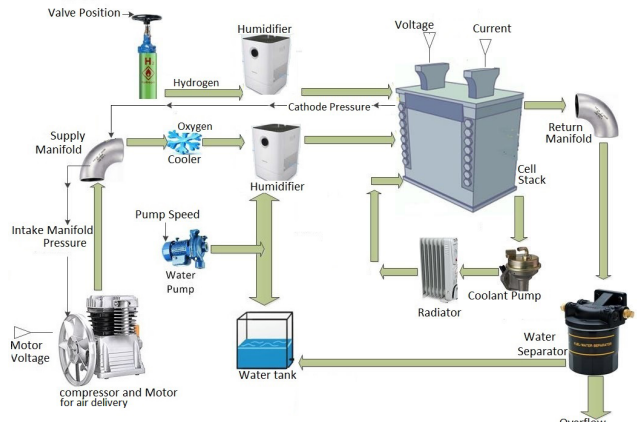


FIGURE 2. Block diagram of a fuel cell.

properties above 80 °C, rigorous fuel cross-over distortions and higher price tag. Research community is putting sustained efforts to overcome these issues [17]–[22]. Energy is produced as a result of a chemical reaction in fuel cell and since no moving parts are involved, the peak efficiency is not limited by Carnot cycle. Unlike dry or acid batteries, fuel cells keep on producing electricity unless or until supply of fuel is not halted. Thus, fuel cells are a source of eco-friendly energy.

In fuel cells, clean and efficient high density electric energy is produced by means of a chemical reaction. Fuel cells are thought to be future of renewable energy source replacing the fossil fuels. Hydrogen in its molecular state provides the highest energy of 143 MJ kg^{-1} among all the known gaseous fuels and is therefore used as a fuel [23]. There are multiple subsystems in a fuel cell which are interconnected with one another so that, the whole system can operate in a smooth manner. The four main subsystems of a PEMFC are listed as follows:

- Fuel supply management system
- Heat management system
- Humidity management system
- Power management system

Fault analysis for humidity management is presented in [24]. During random variations in load requirements in real time scenarios, the demand of reactants increases or decreases. If this demand for the reactants does not meet the actual requirements, then there is a danger of fuel or oxygen starvation or excess can damage the cell stack consequently reducing the life span of the system. Control design is proposed to maintain the desired value of oxygen excess ratio of 2 in order to ensure smooth power delivery and to maintain a constant stack voltage for the desired circumstances. Detailed block diagram of PEMFC is shown in Figure 2. Oxygen excess ratio of the fuel cell stack must be kept constant because if it fluctuates above or below the

reference value, it degrades the overall system performance and can cause damage to the stack. Non-linear control techniques have the potential to stabilize the oxygen excess ratio of the system and to regulate fuel cell power and stack voltage. Also, there is an effect of ambient temperature which plays a vital role in the system performance and control techniques can be applied to minimize the effect of ambient temperature on oxygen excess ratio in order to ensure smooth power delivery. A robust control solution using second order SMC for a laboratory based fuel cell test station has been presented in [25] to solve air delivery problem. Also observer based second order SMC with adaptive gain has been implemented to control the air feed system of a PEM fuel cell with Lipschitz non-linearities in [26].

The remaining paper is organized as follows: The nine state model developed by Pukrushpan is discussed in section II. The control objective of maintaining the oxygen excess ratio λ_{O_2} at a certain threshold is explained in section III. First order Sliding Mode Controller (SMC) and second order SMC are derived in IV and the comparative performance analysis is discussed in section V. Finally the conclusion is presented in section VI.

II. MATHEMATICAL MODEL

The PEM fuel cell is a standard 9th order non-linear system developed by Pukrushpan [27]. The state variables involved in the state equations are as follows:

x_1 is the mass of oxygen inside the fuel cell stack. It is function of oxygen exiting the cathode, utilized in fuel cell.

x_2 is the mass of nitrogen gas in the fuel cell stack, which is a function of nitrogen entering into the cathode and coming out of cathode.

x_3 is the mass of hydrogen in anode. It is also a function of hydrogen entering at anode, exiting from anode and hydrogen reacted at cathode.

x_4 is the speed of compressors motor that supplies air to the fuel cell stack through supply manifold.

x_5 is the pressure at supply manifold. It is a function of partial pressure of gases present in the air. x_6 is the mass of air present in the supply manifold, which is the sum of oxygen, nitrogen and water in the form of vapors present in air.

x_7 is the mass of water at anode. Hydrogen gas is passed through a humidifier to control the embrace humidity. The membrane must be properly humidified such that the stack doesn't either dry out or become flooded by water.

x_8 is the mass of water at cathode. Air is also passed through a humidifier to control the stack's humidity. Water is also produced at cathode due to chemical reaction occurring there. This state shows the dynamic behavior of water at cathode.

x_9 is pressure at return manifold. It consists of partial pressures of gases present in the air that did not take part in chemical reaction. The control input to the system is the voltage given to the compressor motor.

After using some approximations the simplified plant is given by the following nine state space equations

$$\begin{aligned} \dot{x}_1 &= a_1 \left[1 + \frac{a_2 a_4}{x_5 - x_5 a_{10} + a_3} \right]^{-1} \left[k_{sm,out}(x_5 - a_6 x_1 - a_7 x_3 \right. \\ &\quad \left. - a_8 m_{v,ca}) \left(1 + \frac{a_9 a_{10} x_5}{x_5 - x_5 a_{10}} \right)^{-1} \right] \left(1 + \frac{a_9 a_5}{x_5 - a_{10} x_5} \right) \\ &\quad - \left[\left(\frac{a_6 M_{O_2} x_1}{a_6 x_1 + a_7 x_3} \right) \left(\frac{a_6 M_{O_2} x_1}{a_6 x_1 + a_7 x_3} + \left(1 - \frac{a_6 M_{O_2} x_1}{a_6 x_1 + a_7 x_3} \right) \right. \right. \\ &\quad \times M_{N_2} \left. \right)^{-1} k_{ca,out}(a_6 x_1 + a_7 x_3 + a_8 m_{v,ca} - x_9) \\ &\quad \times \left[1 + \left(\frac{M_v a_8 m_{v,ca}}{a_6 x_1 + a_7 x_3} \right) \times \left(\frac{a_6 M_{O_2} x_1}{a_6 x_1 + a_7 x_3} \right. \right. \\ &\quad \left. \left. + \left(1 - \frac{a_6 M_{O_2} x_1}{a_6 x_1 + a_7 x_3} \right) M_{N_2} \right)^{-1} \right]^{-1} \right] - a_{11} I_{st} \end{aligned} \quad (1)$$

$$\begin{aligned} \dot{x}_2 &= \left(1 + \frac{a_{12} a_{13}}{a_{15} x_2 + a_{14} m_{v,an}} \right)^{-1} [k_1 k_2 x_5 - k_1 a_{15} x_2 \\ &\quad - k_1 a_{14} m_{v,an}] - a_{16} I_{st} \end{aligned} \quad (2)$$

$$\begin{aligned} \dot{x}_3 &= (1 - a_1) \left[1 + \frac{a_2 a_4}{x_5 - x_5 a_{10} + a_3} \right]^{-1} \left[k_{sm,out}(x_5 \right. \\ &\quad \left. - a_6 x_1 - a_7 x_3 - a_8 m_{v,ca}) \left(1 + \frac{a_9 a_{10} x_5}{x_5 - x_5 a_{10}} \right)^{-1} \right. \\ &\quad \times \left. \left(1 + \frac{a_9 a_5}{x_5 - a_{10} x_5} \right) \right] - \left[1 - \left[\left(\frac{a_6 M_{O_2} x_1}{a_6 x_1 + a_7 x_3} \right) \right. \right. \\ &\quad \times \left(\frac{a_6 M_{O_2} x_1}{a_6 x_1 + a_7 x_3} + \left(1 - \frac{a_6 M_{O_2} x_1}{a_6 x_1 + a_7 x_3} \right) M_{N_2} \right)^{-1} \\ &\quad \times k_{ca,out}(a_6 x_1 + a_7 x_3 + a_8 m_{v,ca} \\ &\quad - x_9) \left[1 + \left(\frac{M_v a_8 m_{v,ca}}{a_6 x_1 + a_7 x_3} \right) \times \left(\frac{a_6 M_{O_2} x_1}{a_6 x_1 + a_7 x_3} \right. \right. \\ &\quad \left. \left. + \left(1 - \frac{a_6 M_{O_2} x_1}{a_6 x_1 + a_7 x_3} \right) M_{N_2} \right)^{-1} \right]^{-1} \right] \end{aligned} \quad (3)$$

$$\begin{aligned} \dot{x}_4 &= \frac{a_{25} u^2}{x_4} - a_{26} u - a_{27} \left[\left(\frac{x_5}{p_{atm}} \right)^{a_{24}} - 1 \right] \\ &\quad \times \left[a_{22} x_4 - a_{22} x_4 e^{\frac{a_{23}}{x_4^2} \left[\left(\frac{x_5}{p_{atm}} \right)^{a_{24}} - 1 \right] - \beta} \right] \end{aligned} \quad (4)$$

$$\begin{aligned} \dot{x}_5 &= a_{29} a_{22} x_4 \left[1 + \frac{1}{\eta_{cp}} \left[\left(\frac{x_5}{p_{atm}} \right)^{a_{24}} - 1 \right] \right. \\ &\quad \left. - e^{\frac{a_{23}}{x_4^2} \left[\left(\frac{x_5}{p_{atm}} \right)^{a_{24}} - 1 \right] - \beta} \right. \\ &\quad \left. - \left[\frac{e^{\frac{a_{23}}{x_4^2} \left[\left(\frac{x_5}{p_{atm}} \right)^{a_{24}} - 1 \right] - \beta}}{\eta_{cp}} \right. \right. \\ &\quad \times \left[\left(\frac{x_5}{p_{atm}} \right)^{a_{24}} - 1 \right] \left. \right] - \frac{a_{30} x_5}{x_6} [x_5 - a_6 x_1 \\ &\quad - a_7 x_3 - a_8 m_{v,ca}] \end{aligned} \quad (5)$$

$$\begin{aligned} \dot{x}_6 &= a_{22} x_4 - a_{22} x_4 e^{\frac{a_{23}}{x_4^2} \left[\left(\frac{x_5}{p_{atm}} \right)^{a_{24}} - 1 \right] - \beta} \\ &\quad - k_{sm,out} \times (x_5 - a_6 x_1 - a_7 x_3 - a_8 m_{v,ca}) \end{aligned} \quad (6)$$

$$\begin{aligned} \dot{x}_7 &= \left(1 - \left(1 + \frac{a_{12} a_{13}}{a_{15} x_2 + a_{14} m_{v,an}} \right)^{-1} \right) (k_1 k_2 x_5 - k_1 a_{15} x_2 \\ &\quad - k_1 a_{14} m_{v,an}) - (a_{19} I_{st} - a_{20} (\lambda_{ca} - \lambda_{an})) \end{aligned} \quad (7)$$

TABLE 1. Coefficients defined in the fuel cell.

$$\begin{aligned}
a_1 &= x_{O_2,ca,in} \\
a_3 &= \phi^{des} p_{sat,T_{cl}} - \phi_{ca,in} p_{sat,T_{cl}} \\
a_5 &= \phi^{des} p_{sat,T_{cl}} \\
a_7 &= \frac{R_{N_2} T_{st}}{V_{ca}} \\
a_9 &= \frac{M_v}{M_a} \\
a_{11} &= \frac{M_{O_2} n}{4F} \\
a_{13} &= p_{v,ca,in} = \phi_{ca,in} p_{sat,T_{cl}} \\
a_{15} &= \frac{R_{H_2} T_{st}}{V_{in} n} \\
a_{17} &= \frac{V_{in} n}{2F} \\
a_{19} &= \frac{n_d}{A_{fc} F} \\
a_{21} &= M_v A_{fc} n \\
a_{23} &= \frac{\beta 2 C_p T_{cp,in}}{K_{uc}^2 \psi_{max}} \\
a_{25} &= \frac{\eta_{cm}}{J_{cp} R_{cm}} \\
a_{27} &= \frac{e f_{mea} \eta_{cp} J_{cp}}{\gamma R_a T_{atm}} \\
a_{29} &= \frac{V_{sm}}{R_o T_{rm}} \\
a_{31} &= \frac{R_o T_{rm}}{V_{rm}}
\end{aligned}
\quad
\begin{aligned}
a_2 &= \frac{M_v}{M_{a,ca,in}} \\
a_4 &= \phi_{ca,in} p_{sat,T_{cl}} \\
a_6 &= \frac{R_{O_2} T_{st}}{V_{ca}} \\
a_8 &= \frac{R_o T_{st}}{V_{ca}} \\
a_{10} &= \frac{p_{atm}}{\phi_{atm} p_{sat,T_{atm}}} \\
a_{12} &= \frac{M_v}{M_{H_2}} \\
a_{14} &= \frac{R_v T_{st}}{V_{an} n} \\
a_{16} &= \frac{M_{H_2} n}{2F} \\
a_{18} &= \frac{\rho_{m,dry}}{M_{m,dry}} \\
a_{20} &= \frac{D_w a_{18}}{t_m} \\
a_{22} &= \frac{\Phi_{max} \rho \pi d_u K_{uc} \delta}{4 \theta^{0.5}} \\
a_{24} &= \frac{\gamma - 1}{\gamma} \\
a_{26} &= \frac{\eta_{cm} k_v}{J_{cp} R_{cm}} \\
a_{28} &= a_{23} \left(\frac{1}{p_{atm}} \right)^{a_{24}} \\
a_{30} &= k_{sm,out} \gamma \\
a_{32} &= \frac{C_{D,rm} A_{T,rm}}{\sqrt{R_{T,rm}}}
\end{aligned}$$

$$\begin{aligned}
\dot{x}_8 &= \left(1 - \left(1 + \frac{a_2 a_4}{x_5 - x_5 a_{10} + a_3} \right)^{-1} \right) \left[k_{sm,out} (x_5 - a_6 x_1 - a_7 x_3 - a_8 m_{v,ca}) \left(1 + \frac{a_9 a_{10} x_5}{x_5 - x_5 a_{10}} \right)^{-1} \times \left(1 + \frac{a_9 a_5}{x_5 - a_{10} x_5} \right) \right] - \left(1 - \left(1 + \left(\frac{M_v a_8 m_{v,ca}}{a_6 x_1 + a_7 x_3} \right) \times \left(\frac{a_6 M_{O_2} x_1}{a_6 x_1 + a_7 x_3} + \left(1 - \frac{a_6 M_{O_2} x_1}{a_6 x_1 + a_7 x_3} \right) M_{N_2} \right)^{-1} \right)^{-1} \right) \times k_{ca,out} (a_6 x_1 + a_7 x_3 + a_8 m_{v,ca} - x_9) \quad (8)
\end{aligned}$$

$$\dot{x}_9 = a_{31} [k_{ca,out} (a_6 x_1 + a_7 x_3 + a_8 m_{v,ca} - x_9) - W_{rm,out}] \quad (9)$$

The variables involved in the state space equations are as follows, also the constants involved in state equations are defined in Table. 1, where the values of used constants can be seen in [28].

$$\lambda_m = \begin{cases} 0.043 + 17.81 a_i - 39.85 a_i^2 + 36 a_i^2 & 0 < a_i \leq 1 \\ 14 + 1.4(a_i - 1) & 1 < a_i \leq 3 \end{cases}$$

and also,

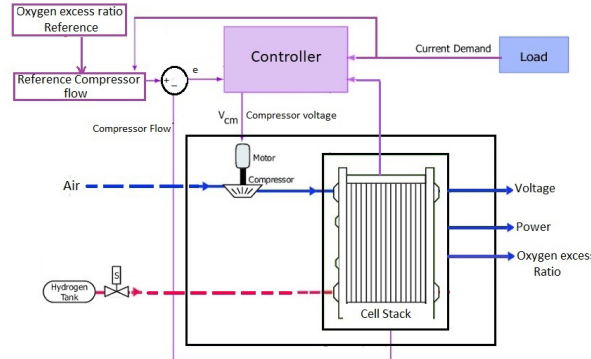
$$W_{rm,out} = a_{32} x_9 \left(\frac{p_{atm}}{x_9} \right)^{\frac{1}{2}} \left[\frac{2\gamma}{\gamma - 1} \left[1 - \left(\frac{p_{atm}}{x_9} \right)^{\frac{\gamma-1}{\gamma}} \right] \right]^{\frac{1}{2}} \quad \text{for } \frac{p_{atm}}{x_9} > \left(\frac{2}{\gamma + 1} \right)^{\frac{\gamma}{\gamma-1}}$$

and

$$W_{rm,out} = a_{32} x_9 \gamma^{\frac{1}{2}} \left(\frac{2}{\gamma + 1} \right)^{\frac{\gamma+1}{2(\gamma-1)}} \quad \text{for } \frac{p_{atm}}{x_9} \leq \left(\frac{2}{\gamma + 1} \right)^{\frac{\gamma}{\gamma-1}}$$

III. CONTROL OBJECTIVES

From control perspective, there are several subsystems in a fuel cell that need proper management including fuel supply subsystem, air flow subsystem, temperature and humidity management systems. In the present work, the temperature of the fuel cell is assumed to be precisely controlled by a perfect

**FIGURE 3.** Block diagram of air delivery system in a PEM fuel cell.

cooling system. It is also assumed that the cell stack is always fully humidified by a perfect humidifier.

The fuel supply subsystem requires that the pressure at anode and cathode are same. This pressure is controlled by a valve. In our model, proportional feedback control ensures that the anode pressure follows the minor changes in cathode pressure. The air supply subsystem also needs special attention to improve the efficiency and to increase the life span of a fuel cell. Decreased air flow leads to oxygen starvation which in-turn results in reduced power and decreased life of the fuel cell. On the other hand, increased air flow causes too much vapor production and the cells can get flooded and the membrane may be damaged. The desired air pressure is maintained by controlling the compressor air flow. A nonlinear control strategy is required to control the air flow of the system. The block diagram for air delivery system is shown in figure 3. The overall control objective is to design the motor compressor voltage to maintain the oxygen excess ratio (λ_{O_2}) at the desired level. It can be defined as

$$\lambda_{O_2} = \frac{W_{O_2,in}}{W_{O_2,react}} \quad (10)$$

To meet the power demand of a fuel cell, oxygen excess ratio must be maintained at $\lambda_{O_2} = 2$ [28]. The control objective can be described as follows;

$$\begin{aligned}
\dot{x} &= f(x, u, w) \\
x &= [m_{O_2} \ m_{N_2} \ m_{H_2} \ \omega_{cp} \ p_{sm} \ m_{sm} \ m_{wan} \ m_{wca} \ p_{rm}] \\
u &= V_{cm} \\
w &= I_{st} \quad (11)
\end{aligned}$$

The outputs of the system include the compressor flow, pressure at supply manifold and stack voltage, i.e.

$$y = [W_{cp} \ p_{sm} \ V_{st}] \quad (12)$$

The performance variables are net power and oxygen excess ratio.

$$z = [P_{net} \ \lambda_{O_2} \ V_{st}] \quad (13)$$

IV. CONTROL DESIGN

First order SMC and second order SMC with super twisting algorithm have been designed to maintain the oxygen excess

ratio at the desired level. Oxygen excess can be controlled by regulating the oxygen inlet flow which is not directly measureable, so compressor speed (ω_{cp}), is used instead to control the oxygen excess ratio.

The objective can be achieved by defining a sliding surface as 14

$$S(x, t) = W_{cp} - W_{cp,ref} \quad (14)$$

where mass flow reference ($W_{cp,ref}$) can be found from oxygen flow reference at cathode ($W_{O_2,ca,ref}$). The required mass flow of dry air ($W_{dry,ref}$) can be given as

$$W_{dry,ref} = \frac{1}{x_{O_2}} W_{O_2,ca,ref} = \frac{1}{x_{O_2}} \lambda_{O_2,ref} M_{O_2} \frac{nI_{st}}{4F} \quad (15)$$

where x_{O_2} is the mass fraction of oxygen, n is the number of cells in the stack, F is the Faradays constant, I_{st} is the stack current, and M_{O_2} is the molar mass of oxygen. Considering the relative humidity of air, the required flow rate of air can be given as

$$W_{cp,ref} = (1 + \omega_{amb}) \frac{1}{x_{O_2}} \lambda_{O_2,ref} M_{O_2} \frac{nI_{st}}{4F} \quad (16)$$

So, the sliding surface can be defined as follows

$$s(x, t) = b_{11}(1 - d(x))x_1 - (1 + \omega_{amb}) \frac{1}{x_{O_2}} \lambda_{O_2,ref} M_{O_2} \frac{nI_{st}}{4F} \quad (17)$$

where b_{11} is a constant and its value is 0.005139, $d(x)$ is a function of x_2 and ω_{amb} is the water vapour constant for ambient conditions.

A. FIRST ORDER SMC

Sliding mode control is a nonlinear control technique and has a remarkable performance against uncertainties [29]. The main objective of SMC is to let the output variable track a desired trajectory [30]. First of all we define a sliding mode function as in (18)

$$S = ce(t) + \dot{e}(t) \quad (18)$$

where e is the tracking error and c is a tuning parameter which must satisfy the Hurwitz condition, $c > 0$. In this particular case, the relative degree is 1 so we define $s = e(t)$. The continuous control part is obtained by taking the first order time derivative of the sliding function [31]. With the assumption that atmospheric pressure and temperature are kept constant. So

$$\dot{S} = au^2 + bu + c \quad (19)$$

where

$$a = [a_{22} - a_{22}e^{\frac{a_{23}}{x_4}((\frac{x_5}{p_{atm}})^{a_{24}}-1)-\beta} + \frac{2a_{22}a_{23}}{p_{atm}^{a_{24}}} \\ \times e^{\frac{a_{23}}{x_4}((\frac{x_5}{p_{atm}})^{a_{24}}-1)-\beta} x_5^3 x_4^{-2} \\ - 2a_{22}a_{23}e^{\frac{a_{23}}{x_4}((\frac{x_5}{p_{atm}})^{a_{24}}-1)-\beta} x_4^{-2}]c_4 x_4^{-1} \quad (20)$$

$$b = -a_{26}[a_{22} - a_{22}e^{\frac{a_{23}}{x_4}((\frac{x_5}{p_{atm}})^{a_{24}}-1)-\beta} + \frac{2a_{22}a_{23}}{p_{atm}^{a_{24}}} \\ \times e^{\frac{a_{23}}{x_4}((\frac{x_5}{p_{atm}})^{a_{24}}-1)-\beta} x_5^3 x_4^{-2} - 2a_{22}a_{23} \\ \times e^{\frac{a_{23}}{x_4}((\frac{x_5}{p_{atm}})^{a_{24}}-1)-\beta} x_4^{-2}] \quad (21)$$

$$c = -[a_{22} - a_{22}e^{\frac{a_{23}}{x_4}((\frac{x_5}{p_{atm}})^{a_{24}}-1)-\beta} + \frac{2a_{22}a_{23}}{p_{atm}^{a_{24}}} \\ \times e^{\frac{a_{23}}{x_4}((\frac{x_5}{p_{atm}})^{a_{24}}-1)-\beta} x_5^3 x_4^{-2} - 2a_{22}a_{23} \\ \times e^{\frac{a_{23}}{x_4}((\frac{x_5}{p_{atm}})^{a_{24}}-1)-\beta} x_4^{-2}]a_{27}[(\frac{x_5}{p_{atm}})^{a_{24}} - 1] \\ \times [a_{22}x_4 - a_{22}x_4[e^{\frac{a_{23}}{x_4}((\frac{x_5}{p_{atm}})^{a_{24}}-1)-\beta}]] \\ - (\frac{a_{22}a_{23}a_{24}e^{\frac{a_{23}}{x_4}((\frac{x_5}{p_{atm}})^{a_{24}}-1)-\beta} x_4^{-1} x_5^{a_{24}-1}}{p_{atm}^{a_{24}}}) \\ \times \left(a_{29}a_{22}x_4[1 + \frac{1}{\eta_{cp}}(\frac{x_5}{p_{atm}})^{a_{24}} - 1)] \right. \\ \left. - e^{\frac{a_{23}}{x_4}((\frac{x_5}{p_{atm}})^{a_{24}}-1)-\beta} \right. \\ \left. - e^{\frac{a_{23}}{x_4}((\frac{x_5}{p_{atm}})^{a_{24}}-1)-\beta} \right. \\ \left. - \frac{e^{\frac{a_{23}}{x_4}((\frac{x_5}{p_{atm}})^{a_{24}}-1)-\beta}}{\eta_{cp}} ((\frac{x_5}{p_{atm}})^{a_{24}} - 1) \right. \\ \left. - a_{30}\frac{x_5}{x_6}[x_5 - a_6x_1 - a_7x_3 - a_8m_{v,ca}] \right) - 2.8 \\ \times 10^{-2}d \frac{dI_{st}}{dt} \quad (22)$$

Using quadratic formula, the continuous part of the control input can be given as

$$u_{eq(1,2)} = \frac{-b \pm \sqrt{b^2 - 4ac}}{2a} \quad (23)$$

The discontinuous control part can be written as

$$u_{dis} = -K \text{Sign}(s) \quad (24)$$

The overall first order SMC based law can be given as

$$u = u_{eq} + u_{dis} \quad (25)$$

B. EXISTENCE OF SLIDING MODE

The existence of SMC can be proved by evaluating lyapunov stability [32] as follows;

$$V = \frac{1}{2}S^2$$

$$\dot{V} = S\dot{S} = S(au^2 + bu + c)$$

where,

$$u = \frac{-b + \sqrt{b^2 - 4ac}}{2a} - K \text{Sign}(S)$$

After substituting the values, we get

$$\dot{V} = S[0 - K \text{Sign}(S)]$$

$$\dot{V} \leq S(-K|S|)$$

$$\dot{V} \leq -KS^2$$

It shows that $\dot{V} \leq 0$, $\forall K > 0$ which proves asymptotic stability ensuring the existence of SMC.

C. SECOND ORDER SMC

In the second order SMC, the sliding surface S does not directly depend upon control input u . However u appears in the first derivative of S showing the relative degree of system as 1 i.e.

$$\dot{s}(x, t) = \frac{\partial s}{\partial t} + L_f s + L_g s u \quad (26)$$

Since $L_g s(x, t) \neq 0$ and also, the vector field f & g are smooth. Since the relative degree of the sliding variable is 1 w.r.t. u . A conventional first order SMC can easily be implemented. However this controller will not achieve the desired results in case of a fuel cell, because It would affect the net output power of the system which has relative degree 0 w.r.t. u . Thus, Second order SMC based law provides an alternative to this problem since it has the potential to achieve smooth output thus preventing the net output power loss of the system [33]. Differentiating the sliding variable twice gives the following expression

$$\ddot{s}(t) = \varphi(t, x, u) + \gamma(t, x, u)\dot{u}(t) \quad (27)$$

where

$$\gamma(t, x, u) = L_g \dot{s}(x, t) \quad (28)$$

and

$$\varphi(t, x, u) = L_f \dot{s}(x, t) + L_g \dot{s}(x, t) \quad (29)$$

These functions $\gamma(t, x, u)$ & $\varphi(t, x, u)$ can be globally bounded as follows

$$0 < \Gamma_m \leq \gamma(t, x, u) \leq \Gamma_M \quad (30)$$

$$|\varphi(t, x, u)| \leq \Phi \quad (31)$$

Considering $s_0 = 5e^{-4}$, after complex mathematical computations, following bounds on $\gamma(t, x, u)$ & $\varphi(t, x, u)$ have been determined

$$\Gamma_m = 0.5, \quad \Gamma_M = 0.9, \quad \Phi = 0.01$$

Knowing the bounds, the stabilization problem of a fuel cell system with MIMO dynamics can be resolved by solving the given differential equation by application of second order SMC.

$$\ddot{s} \in [-0.01, 0.01] + [0.5, 0.9]\dot{u} \quad (32)$$

Using these global bounds on functions $\gamma(t, x, u)$ and $\varphi(t, x, u)$, the control parameters can be defined easily.

1) SUPER TWISTING ALGORITHM

This algorithm has been specially designed for systems with relative degree as 1. Its prominent feature is that it does not need any information about \dot{s} during operation. It consists of two terms; First one is the integral of a discontinuous function and the second one is the continuous function of s . The control input, as defined by A. Levant in [34] can be written as

$$u(t) = u_1(t) + u_2(t)$$

$$\dot{u}_1(t) = -\gamma \operatorname{sign}(s)$$

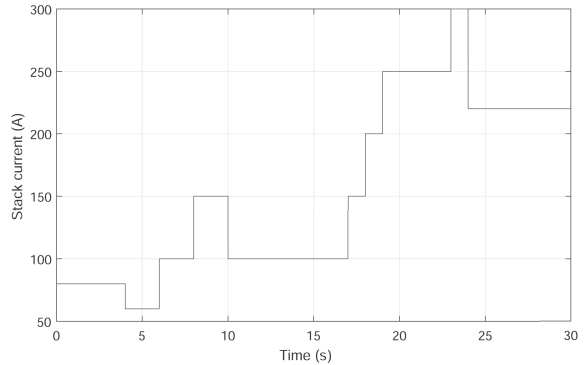


FIGURE 4. Stack current created from step functions.

$$u_2(t) = -\lambda |s_0|^\rho \operatorname{sign}(s) \quad (33)$$

where λ , ρ and γ in the control equation are the design parameters. The bounds on these parameters are given by

$$\begin{aligned} \gamma &> \frac{\Phi}{\Gamma_m} \\ \lambda^2 &\geq \frac{4\Phi}{\Gamma_m^2} \frac{\Gamma_M(\gamma + \Phi)}{\Gamma_m(\gamma - \Phi)} \\ 0 &< \rho \leq 0.5 \end{aligned} \quad (34)$$

These control parameters must be designed by keeping in view the overall behavior of a fuel cell that includes output power and oxygen excess ratio. After fine tuning, following parameters are obtained

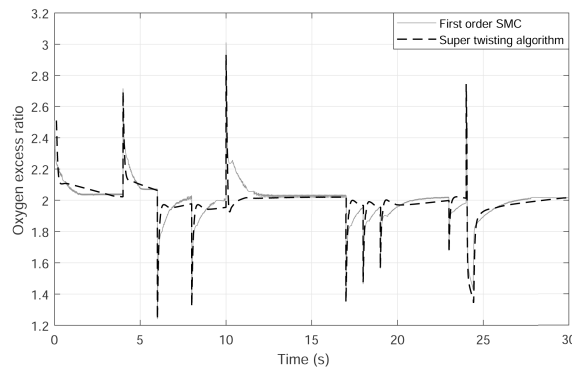
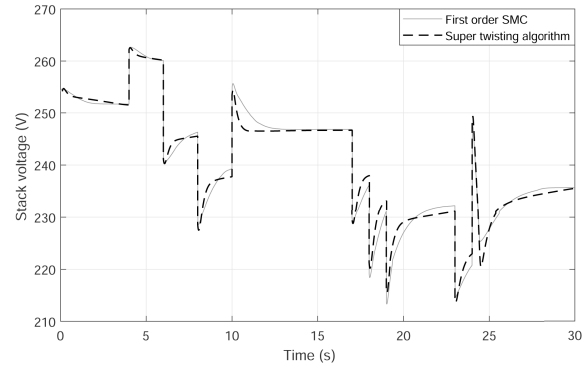
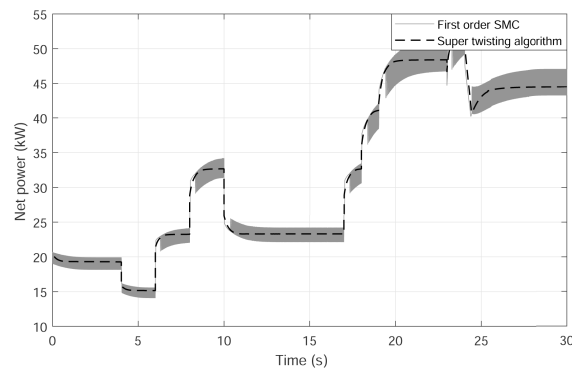
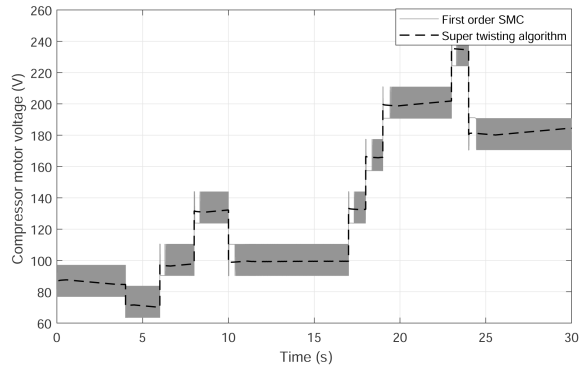
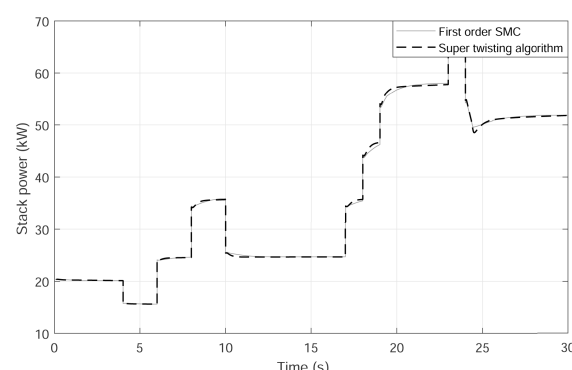
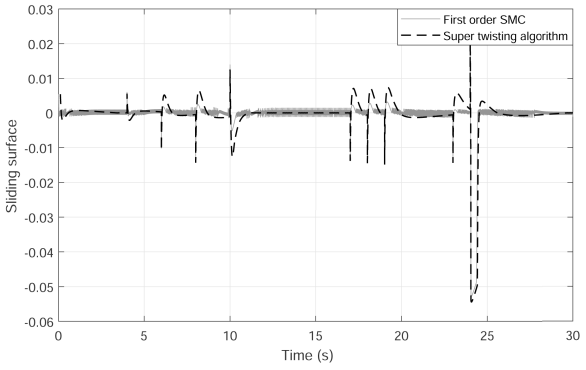
$$\gamma = 2, \quad \lambda = 2, \quad \rho = 0.5$$

V. RESULTS AND DISCUSSION

Simulations on ninth order plant model are conducted in MATLAB/Simulink environment running on a laptop having Intel core i5 processor. The objective is to analyze the performance of the designed first order SMC and second order SMC with super twisting algorithm and to observe controllers' behavior for oxygen excess ratio, stack voltage and the generated power in the presence of model uncertainties and disturbances along variety of power demands. A disturbance current ranging from 60A to 300A shown in Figure 4 is considered as disturbance input which is demanded by the fuel cell. Sudden variations in current demand act as a disturbance and compressor motor voltage has to be adjusted accordingly to ensure that smooth power delivery.

A. SIMULATION RESULTS

The reference value for oxygen excess ratio is taken as 2 and sudden variations in input current are applied in simulation. Results indicate that smooth power delivery can be achieved by keeping the oxygen excess ratio constant while ensuring tracking. Figure 5 shows the comparative performance achieved by the two controllers. Results clearly indicate that super twisting algorithm outperforms the first order SMC. First order SMC has some chattering in the curve of oxygen excess ratio whereas the results obtained using super

**FIGURE 5.** Oxygen excess ratio.**FIGURE 8.** Stack voltage produced by fuel cell.**FIGURE 6.** Net power produced by fuel cell.**FIGURE 9.** Compressor motor voltage.**FIGURE 7.** Stack power produced by fuel cell.**FIGURE 10.** Sliding surface or the error signal.

twisting algorithm are much smoother. Smooth signal to the compressor motor ensures a smooth operation of the fuel cell system. The graph shown in Figure 6 presents the total power generated by the fuel cell stack. The compressor motor is acting as a load to the fuel cell, thus the net power is the difference of the stack power and the power consumed by the compressor. Result show that transient response of power is improved with super twisting algorithm as compared to first order SMC. Similarly, the stack power generated by the fuel cell is shown in Figure 7. The behavior of the net stack voltage produced by the fuel cell is shown in Figure 8. It shows that first order SMC suffers from chattering in power curve.

When super twisting algorithm is applied, the problem of chattering is resolved and smooth voltage curve is obtained. Thus, it can be concluded that using super twisting algorithm, a uniform voltage can be provided to a certain load which is being driven by a fuel cell. The transient time plot of the sliding surface which is also the error signal in this particular case indicates that the controller minimizes the difference between the actual and desired air flows i.e. $S(t) = 0$. The sliding surface is shown in Figure 10. The compressor motor voltage which controls the whole process for maintaining a balanced oxygen excess ratio and hence ensures a smooth power delivery is shown in Figure 9. Comparing both the curves, we can conclude that super twisting algorithm has less fluctuations which in turn will increase the life span of the motor. The controller outputs for both the designed

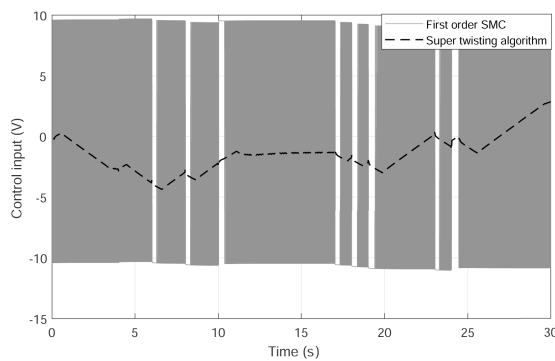


FIGURE 11. Control input.

control laws is compared in Figure 11. The figure clearly shows that the output signal of the controller using super twisting algorithm demonstrates less chattering as compared to first order SMC. Thus, it can be concluded that using super twisting algorithm, there will be less stress on compressor motor.

VI. CONCLUSION

This research investigates the strategies to improve the transient response and steady state behavior of a PEMFC. The main objective is to present the design and successful application of non-linear control on the fuel cell. Two variants of SMC laws have been developed to control various states of the fuel cell. The control performance of both control laws to regulate various parameters has been evaluated in simulation. Results demonstrate that PEMFC when subjected to second order SMC exhibits better transient response under disturbances in comparison with first order SMC. It also ensures smooth power delivery and offers less chattering in the signals corresponding to control input and compressor motor voltage. The comparison of oxygen excess ratio in both cases indicates that the controller using super twisting algorithm has no jittering.

A. NOMENCLATURE

<i>c</i>	Concentration
<i>F</i>	Faradays constant
<i>M</i>	Molar mass
<i>i</i>	Stack current density
<i>J</i>	Inertia
<i>K</i>	Restriction constant
λ	Water content
<i>an</i>	Anode
<i>w</i>	Water
<i>H</i> ₂	Hydrogen
<i>m</i>	Memberane
<i>cp</i>	Compressor motor
<i>hum</i>	Humidifier air
<i>net</i>	Total
<i>rm</i>	Return manifold
<i>N</i> ₂	Nitrogen

<i>sm</i>	Supply manifold
<i>ref</i>	Reference
<i>D</i>	Diffusion coefficient
<i>E</i>	Nernst voltage of a PEMFC
<i>P</i>	Pressure
<i>I</i>	Current
γ	Specific heat ratio
<i>n</i>	Number of fuel cells in stack
<i>ca</i>	Cathode
<i>a</i>	Air
<i>O</i> ₂	Oxygen
<i>st</i>	Stack
<i>out</i>	Output / Exiting
<i>v</i>	Water vapour
<i>react</i>	Consumed in reaction
<i>amb</i>	Ambient
<i>sat</i>	Saturation
<i>in</i>	Entering / input

REFERENCES

- [1] L. Pérez-Lombard, J. Ortiz, and C. Pout, “A review on buildings energy consumption information,” *Energy Buildings*, vol. 40, no. 3, pp. 394–398, Jan. 2008.
- [2] R. Lenoir-Improtta, pp. Devine-Wright, J. Q. Pinheiro, and P. Schweizer-Ries, “Energy issues: Psychological aspects,” in *Handbook of Environmental Psychology and Quality of Life Research*. Cham, Switzerland: Springer, 2017, pp. 543–557.
- [3] C. A. Hall, “Fossil fuels,” in *Energy Return Investment*. Cham, Switzerland: Springer, 2017, pp. 95–105.
- [4] H. M. Quested, J. H. C. Cornelissen, M. C. Press, T. V. Callaghan, R. Aerts, F. Trosien, P. Riemann, D. Gwynn-Jones, A. Kondratchuk, and S. E. Jonasson, “Decomposition of sub-arctic plants with differing nitrogen economies: A functional role for hemiparasites,” *Ecology*, vol. 84, no. 12, pp. 3209–3221, Dec. 2003.
- [5] F. P. Perera, “Multiple threats to child health from fossil fuel combustion: Impacts of air pollution and climate change,” *Environ. Health Perspect.*, vol. 125, no. 2, pp. 141–148, Feb. 2017.
- [6] M. Ehsani, Y. Gao, and A. Emadi, *Modern Electric, Hybrid Electric, Fuel Cell Vehicles: Fundamentals, Theory, Design*. Boca Raton, FL, USA: CRC Press, 2009.
- [7] R. B. Jackson, P. Friedlingstein, R. M. Andrew, J. G. Canadell, C. L. Quéré, and G. P. Peters, “Persistent fossil fuel growth threatens the paris agreement and planetary health,” *Environ. Res. Lett.*, vol. 14, no. 12, 2019, Art. no. 121001.
- [8] G. T. Kalghati, “Developments in internal combustion engines and implications for combustion science and future transport fuels,” *Proc. Combustion Inst.*, vol. 35, no. 1, pp. 101–115, 2015.
- [9] S. Shafiee and E. Topal, “When will fossil fuel reserves be diminished?” *Energy Policy*, vol. 37, no. 1, pp. 181–189, Jan. 2009.
- [10] S. Jose and S. Archanaa, “Environmental and economic sustainability of algal lipid extractions: An essential approach for the commercialization of algal biofuels,” in *Algal Biofuels*. Cham, Switzerland: Springer, 2017, pp. 281–313.
- [11] M. Cao, Q. Xu, X. Qin, and J. Cai, “Battery energy storage sizing based on a model predictive control strategy with operational constraints to smooth the wind power,” *Int. J. Electr. Power Energy Syst.*, vol. 115, Feb. 2020, Art. no. 105471.
- [12] P. Singh, N. K. Meena, A. Slowik, and S. K. Bishnoi, “Modified african buffalo optimization for strategic integration of battery energy storage in distribution networks,” *IEEE Access*, vol. 8, pp. 14289–14301, 2020.
- [13] S. Simmons and W. Lubitz, “Archimedes screw generators for sustainable energy development,” in *Proc. IEEE Canada Int. Hum. Technol. Conf. (IHTC)*, Jul. 2017, pp. 144–148.

- [14] K. Kim, P. Heo, T. Ko, and J.-C. Lee, “Semi-interpenetrating network electrolyte membranes based on sulfonated poly(arylene ether sulfone) for fuel cells at high temperature and low humidity conditions,” *Electrochim. Commun.*, vol. 48, pp. 44–48, Nov. 2014.
- [15] M. Marrony, R. Barrera, S. Quenet, S. Ginocchio, L. Montelatici, and A. Aslanides, “Durability study and lifetime prediction of baseline proton exchange membrane fuel cell under severe operating conditions,” *J. Power Sources*, vol. 182, no. 2, pp. 469–475, Aug. 2008.
- [16] N. Gallandat, K. Romanowicz, and A. Zättel, “An analytical model for the electrolyser performance derived from materials parameters,” *J. Power Energy Eng.*, vol. 5, no. 10, pp. 34–49, 2017.
- [17] K. Kim, P. Heo, T. Ko, K.-H. Kim, S.-K. Kim, C. Pak, and J.-C. Lee, “Poly(arylene ether sulfone) based semi-interpenetrating polymer network membranes containing cross-linked poly(vinyl phosphonic acid) chains for fuel cell applications at high temperature and low humidity conditions,” *J. Power Sources*, vol. 293, pp. 539–547, Oct. 2015.
- [18] H. Zhang and P. K. Shen, “Recent development of polymer electrolyte membranes for fuel cells,” *Chem. Rev.*, vol. 112, no. 5, pp. 2780–2832, May 2012.
- [19] J. W. Lee, D. Y. Lee, H.-J. Kim, S. Y. Nam, J. J. Choi, J.-Y. Kim, J. H. Jang, E. Cho, S.-K. Kim, and S.-A. Hong, “Synthesis and characterization of acid-doped polybenzimidazole membranes by sol-gel and post-membrane casting method,” *J. Membrane Sci.*, vol. 357, nos. 1–2, pp. 130–133, Jul. 2010.
- [20] K. Jyotheeswara Reddy and N. Sudhakar, “High voltage gain interleaved boost converter with neural network based MPPT controller for fuel cell based electric vehicle applications,” *IEEE Access*, vol. 6, pp. 3899–3908, 2018.
- [21] A. A. Amamou, S. Kelouwani, L. Boulon, and K. Agbossou, “A comprehensive review of solutions and strategies for cold start of automotive proton exchange membrane fuel cells,” *IEEE Access*, vol. 4, pp. 4989–5002, 2016.
- [22] G. Mallesham and C. S. Kumar, “Power quality improvement of weak hybrid pemfc and scig grid using upqc,” in *Advances in Decision Sciences, Image Processing, Security and Computer Vision*. Cham, Switzerland: Springer, 2020, pp. 406–413.
- [23] C. Kunusch, P. Puleston, and M. Mayosky, *Sliding-Mode Control PEM Fuel Cells*. London, U.K.: Springer, 2012.
- [24] J. Liu, Q. Li, H. Yang, Y. Han, S. Jiang, and W. Chen, “Sequence fault diagnosis for PEMFC water management subsystem using deep learning with t-SNE,” *IEEE Access*, vol. 7, pp. 92009–92019, 2019.
- [25] C. Kunusch, P. F. Puleston, M. A. Mayosky, and L. Fridman, “Experimental results applying second order sliding mode control to a PEM fuel cell based system,” *Control Eng. Pract.*, vol. 21, no. 5, pp. 719–726, May 2013.
- [26] S. Laghrouche, J. Liu, F. S. Ahmed, M. Harmouche, and M. Wack, “Adaptive second-order sliding mode observer-based fault reconstruction for PEM fuel cell air-feed system,” *IEEE Trans. Control Syst. Technol.*, vol. 23, no. 3, pp. 1098–1109, May 2015.
- [27] J. T. Pukrushpan, A. G. Stefanopoulou, and H. Peng, *Control of Fuel Cell Power Systems: Principles, Modeling, Analysis and Feedback Design*. Cham, Switzerland: Springer, 2004.
- [28] J. T. Pukrushpan, A. G. Stefanopoulou, and H. Peng, “Control of fuel cell breathing,” *IEEE Control Syst. Mag.*, vol. 24, no. 2, pp. 30–46, Apr. 2004.
- [29] Y. Yun, J. Guo, and S. Tang, “Robust smooth Sliding-Mode-Based controller with fixed-time convergence for missiles considering aerodynamic uncertainty,” *Int. J. Aerosp. Eng.*, vol. 2018, pp. 1–12, Jun. 2018.
- [30] T. Su, X. Liang, G. He, Q. Zhao, and L. Zhao, “Robust trajectory tracking of delta parallel robot using sliding mode control,” in *Proc. IEEE Symp. Ser. Comput. Intell. (SSCI)*, Dec. 2019, pp. 508–512.
- [31] R. Chen, *2011 International Conference in Electrics, Communication and Automatic Control Proceedings*, vol. 165. Springer, 2011.
- [32] J. Liu and X. Wang, *Advanced Sliding Mode Control for Mechanical System*. Springer, 2012.
- [33] K. S. Low, “Design of second order sliding mode controller using smoothening method for machine tools,” Ph.D. dissertation, Dept. Eng. Technol., Tunku Abdul Rahman Univ. College, Kuala Lumpur, Malaysia, 2020.
- [34] A. Levant, “Sliding order and sliding accuracy in sliding mode control,” *Int. J. Control.*, vol. 58, no. 6, pp. 1247–1263, Dec. 1993.



USMAN JAVAID received the B.S. and M.S. degrees in 2009 and 2013, respectively. He is currently pursuing the Ph.D. degree with the Electrical and Computer Engineering Department (ECE), COMSATS University Islamabad, Pakistan. He is also working as a Lecturer. His research interests include electronic fuel injection systems of motorcycles, renewable energy, and non-linear control systems.



ADEEL MEHMOOD received the B.S. degree in mechatronics engineering from the National University of Science and Technology, Pakistan, in 2006, the M.S. degree in robotics and embedded systems from the University of Versailles Saint-Quentin en Yvelines, France, in 2008, and the Ph.D. degree in nonlinear control from the Technical University of Belfort-Montbeliard, France. He worked as a Postdoctoral Researcher with the University of Haute-Alsace, France. He is currently working as an Assistant Professor with COMSATS University Islamabad, Pakistan. His research interests include robotics, renewable energy, and robust and nonlinear control of servo systems.



ALI ARSHAD (Member, IEEE) received the B.E. degree in electrical engineering and the M.S. degree in computer engineering from the University of Engineering and Technology Taxila, Taxila, Pakistan, in 2006 and 2012, respectively, and the Ph.D. degree in electrical engineering from the COMSATS Institute of Information Technology (CIIT), Islamabad, Pakistan, in 2016. He is currently working as an Assistant Professor with the Department of Electrical and Computer Engineering, COMSATS University Islamabad. His current research interests include the control of infinite dimensional systems, sliding mode control theory, modeling and simulation of complex systems, parameter estimation, and mathematical programming.



FAHAD IMTIAZ received the B.Sc. degree in electrical engineering from the Mirpur University of Science and Technology, Azad Kashmir, in 2013, and the M.Sc. degree in electrical engineering from the COMSATS Institute of Information and Technology (CIIT), Islamabad, in 2017. He worked as a Lab Engineer with the Department of Electrical Engineering, Bahria University, Islamabad. He is currently working as a Project Planning and Control Engineer with the Metallurgical Corporation of China, KSA Branch. His research interests include control of polymer electrolyte membrane (PEM) fuel cell systems, renewable energy systems, and robotics.



JAMSHED IQBAL (Senior Member, IEEE) received the Ph.D. degree in robotics from the Italian Institute of Technology (IIT) and the three master's degrees in various fields of engineering from Finland, Sweden, and Pakistan. He is currently working as a Research Associate Professor with the University of Jeddah, Saudi Arabia. With more than 20 years of multi-disciplinary experience in industry and academia, his research interests include robot analysis, and design and control. He has more than 60 journal articles on his credit with H-index of 26.